Oxy-hydrogen, solar and wind assisted hydrogen (H_2) recovery from municipal plastic waste (MPW) and saltwater electrolysis for better environmental systems and ocean cleanup

Linus Onwuemezie , Hamidreza Gohari Darabkhani [1],*

Centre For Renewable and Sustainable Engineering (CRSE), School of Digital, Technology, Innovation and Business (DTIB), Staffordshire University, Stoke-on-Trent, ST4 2DE, UK

ARTICLE INFO

ABSTRACT

The pyrolysis of plastic waste and the electrolysis of saltwater is a promising route to carbon neutrality in ocean cleanup and plastic waste management. Therefore, a solar and wind assisted H_2-fuelled fast pyrolysis of MPW (municipal plastic waste) and electrolysis of desalinated saline were developed. The combined system uses an oxy-hydrogen furnace for thermal decomposition of MPW feed, CO_2 as an inert reaction medium and both solar and wind energy systems to operate the electrical units. The deionised H_2O feed to the electrolyser cell was produced from saltwater using the recovered heat from the fast pyrolyser unit. The process CO_2 was captured and reused for soil improvement as current waste-to-energy routes of MPW recycling emit 695,850 tonnes of CO_2. 2.65 kg/hr_{H_2} fuel in an O_2 environment was utilised to meet the decomposer operating temperature and heat duty which is approximately 29 % of the produced H_2. Instability associated with bio-oil was prevented by using fast pyrolysis which release more volatiles. Compared to the related studies, this investigated work achieved the highest gas and carbon yields. Thermal $NO < 0.1$ ppm was recorded. The developed system is expected to reach ≥ 70 % energy efficiency and a sales price of $< \$3.89/kg_{H_2}$.

Nomenclature

Abbreviations and Symbols	
AEC	Alkaline electrolysis cell
CCS	Carbon capture and storage
HX	Heat exchangers
HDPE	High-density polyethylene
LDPE	Low-density polyethylene
MJ	Megajoule
MW	Megawatt
NO	Nitric oxide
NOx	Nitrogen oxides
OPW	Ocean-bound plastic waste
PEMEC	Proton exchange membrane electrolyser cell
PET	Polyethylene terephthalate
PP	Polypropylene
PS	Polystyrene
PSA	Pressure swing adsorption
PV	Photovoltaic
PVC	Polyvinyl chlorine

1. Introduction

Plastics which are considered synthetic polymers, have influenced global economic growth due to their physical properties (low density, durability and mouldability) and low cost. Global plastics production has increased, reaching 368 million metric tons (Mt) in 2019 and 400 Mt by 2024, with a yearly production of 53 Mt by 2030. As of 2015, 7.82 billion tonnes of plastics were produced [1–3]. Currently, the accumulated plastic waste in the environment is approximately 2.2 gigatonnes (Gt) and is expected to reach 3.1 Gt by 2050 [4]. Without further production of plastics from 2022, micro and plastics in the environment are predicted to reach 2.15 Gt by 2050 because of leakage of the accumulated ones [5]. Apart from landfilled plastic waste, most of the plastic waste also ends up in seas or oceans. For instance, more than 150 million
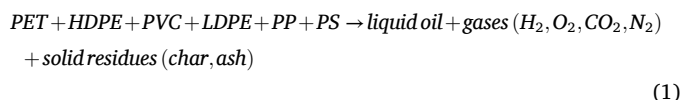
tonnes of plastic waste are in the ocean which endangers marine life and the health of the oceans [6]. At present, about 76 % of plastic waste ends up in landfills. While between 9 % and 12 % are recycled or incinerated. In addition, over 3 % of plastic waste forms ocean-bound plastic waste (OPW) (plastic waste that enters the ocean within 50 km of the seashore) because of mismanagement [4]. Most of the plastic waste that ends up in landfills is transported to the ocean. For instance, between 70 % and 80 % of OPW were transported to seas or oceans by rivers or coastlines as Meijer et al. concluded that approximately 1 million tonnes of plastics in the ocean came from rivers [7,8]. Furthermore, between 20 % and 30 % of OPW comes from abandoned ships, fishing nets, lines and ropes [9]. As of 2010, the United States and EU countries including the former member state (UK) produced the largest amount of plastic waste entering the oceans [10]. Presently, polyethylene terephthalate (PET), high-density polyethylene (HDPE), polyvinyl chlorine (PVC), low-density polyethylene (LDPE), polypropylene (PP) and polystyrene (PS) are the main sources of plastic waste because of increased production globally. For example, in 2015, between 52 and 68 million tonnes of global plastic production come from HDPE, LDPE and PP separately. If this misuse of plastic waste practices continues, marine life will struggle to adapt to the new ecosystem. Thus, 4 major routes for accumulative plastic waste recycling have been established of which re-extrusion is the dominant method. Other recycling routes include mechanical recycling with a single plastic feedstock, chemical recycling using pyrolysis and energy recovery using thermolysis technologies [1]. In contrast to other forms of plastic waste recycling routes, thermolysis with synthetic gas recovery costs less to remove accumulated plastic waste from landfills and oceans. In addition, the recycling of newly plastic waste that has not reached the landfill and ocean through thermolysis routes can reduce landfill space due to China's ban on scrap material imports. For instance, the produced syngas and other by-products like carbon can be sold to recover investment costs and boost profit. Nowadays, pyrolysis and gasification are the two main routes of thermolysis of waste plastic to fuel/energy. The pyrolysis method of producing synthetic gas from plastic waste releases lower carbon emissions in contrast to gasification and is more suitable and efficient compared to the mechanical plastic recycling route for small-scale installations.

Plastic waste pyrolysis which is very similar to biomass pyrolysis, is a thermal and catalytic recycling method of converting waste plastic or organic polymers into gas, liquid oil, and solid residues (charcoal and ash) at reaction temperatures of 500 °C–800 °C [11]. The pyrolysis process of syngas production is grouped into slow and fast reactions. The fast pyrolysis reaction requires heating above 300 °C/min to achieve higher synthesis gas and carbon yields and lower liquid oil production. On the other hand, more char is produced during slow pyrolysis at a reaction temperature below 7 °C/min. Both pyrolysis reaction pathways are operated in a fluidized bed reactor (FBR), entrained flow, batch, circulating fluidized beds or rotating reactors. The FBR is mostly used (dominant), while the rotating reactor is emerging because of the use of optimal temperature (1000 °C/min) leading to a faster heat rate (a few seconds) [12]. Fast pyrolysis of plastic waste treatment was tested on a pilot scale with FBR and showed a promising approach to waste treatment. However, the higher reaction temperature of plastic waste pyrolysis has led to a catalytic process that operates at lower temperatures. For example, the use of a natural zeolite catalyst in the thermal cracking of waste plastics has been found to reduce the amount of liquid oil and impurities such as char, sulphur, nitrogen, and phosphorous formation. In addition, catalytic pyrolysis uses lower operating temperatures which reduces the energy input to produce more gases, unlike the high-temperature pyrolysis process of plastic waste [11,13]. Despite the advantages of catalytic plastic waste pyrolysis such as higher syngas production rate, lower energy input and carbon emission footprints, a mixture of polymers and a catalyst which makes catalyst recovery difficult was reported as one of the major drawbacks. Faster degradation and reduced catalyst activities due to catalyst deposition on polymer pores and carbon emissions have also been reported as disadvantages of catalytic plastic waste pyrolysis [14,15].

For these reasons, two-stage cumulative processes involving thermal decomposition in the initial stage and catalytic cracking in the final stage to increase syngas formation at a lower operating temperature were proposed. Other mitigation approaches include a mixture of plastic waste feedstock, the use of low-carbon fuel and solar thermal such as CSP (concentrating solar power) systems. These suggested approaches will enhance catalyst recovery by preventing catalyst diffusion in large polymer pores and reduce carbon emissions released by burning fossil fuels in the decomposer furnace. For example, Budsaereechai et al. investigated a catalytic pyrolysis of plastic waste using a mixture of PS, PP, LDPE and HDPE as feedstock with a bentonite clay pellets catalyst and reported an increase in calorific value and a decrease in viscosity because of the absence of pressure loss [16]. It was concluded that the use of the reported low-cost pellet catalyst eliminated the pressure drop associated with the powder catalyst, which increased the processing time by 10 min/kg. Nevertheless, catalytic pyrolysis of both biomass and plastic wastes produces higher liquid oil in contrast to fast pyrolysis. The increase in bio-oil production due to lower operating temperature increases the instability of the produced liquid oil because of the deterioration and degradation of the different feedstock properties. Recently, Hassibi et al. [17] investigated the pyrolysis of liquid oil using PP waste as feedstock and kerosene as the benchmark to mitigate instability issues with liquid oil. The findings of the studied work revealed that pyrolyser without reflux is more stable and the stability of liquid oil from the pyrolysis of plastic (PP) waste improved by adding kerosene for long-term storage. The minimal chemical changes and stable pH value of the liquid oil, which improved the stability of the stored liquid oil were promoted by the addition of kerosene [17].

In addition, our previous work investigated the reduction of carbon emissions using a CSP system to produce thermal energy for the pyrolysis of hydrocarbons and biomass systems. From the researched work, it was concluded that replacing the fossil fuel cracking furnace with solar thermal energy and burning H_2 in an O_2 environment (oxy-hydrogen) to meet the activation energy due to losses, and integration of a small-scale CCS unit can eliminate carbon emission footprints as well as improve the overall efficiency [18]. However, the previous study was for large-scale applications due to the involvement of the CSP system and other downstream units. Furthermore, biomass pyrolysis for biochar production has been promoted for soil amendments, capable of mitigating climate change and increasing crop yields and carbon sequestration [19]. Nevertheless, biochar properties in soil for nourishment change over time, causing instability issues. These changes in biochar properties in soils are influenced by the type of feed, operating conditions and the reaction medium used during the production. Unlike N_2 or argon (Ar), CO_2 as one of the reaction mediums provides better biochar stability by preventing the increase of dissolved organic matter (DOM). Instead, further stability analysis of the produced biochar in the CO_2 environment using unmixed biomass or other feed in the pyrolysis process is required. Feeding process CO_2 to the pyrolyser to recover more biochar can prevent carbon emissions into the environment [20,21]. As carbon has the highest share of the pyrolysis of plastic waste by-product, using process CO_2 as a reaction medium and mixing with by-product carbon and ash are worth investigating. Thermal/catalytic pyrolysis of plastic waste by-products is represented in Eq. (1).

$$PET + HDPE + PVC + LDPE + PP + PS \rightarrow liquid\,oil + gases\,(H_2, O_2, CO_2, N_2)$$
$$+ solid\,residues\,(char, ash)$$

$$(1)$$

Other possible approaches to eliminate carbon footprints from small-scale plastic waste pyrolysis are the introduction of an oxy-hydrogen burner, thermal energy recovery to operate downstream units and renewable power systems such as solar PV and wind turbine. H_2 utilisation as a carbon-free fuel in thermal applications has been studied

extensively. For example, Lazaroiu et al. investigated the injection of H_2 fuel into the solid fuel (biomass) furnace for low-carbon emissions and reported a 10 % increase in flame temperature, a 40 % reduction of SO_2 concentration and a 4 % improvement in thermal efficiency. Nevertheless, NOx formation also increased by 10 % because of H_2 involvement in the combustion process [22]. Steam addition instead of N_2 and oxy-hydrogen rather than air-hydrogen combustion have been suggested to minimise NOx formation in high-temperature thermal applications. For instance, oxy-hydrogen furnace for blast furnace – basic oxygen furnace (BF-BOF) was investigated in previous studies and the findings showed lower NOx production, absence of carbon emissions and higher thermal energy efficiency [23]. Apart from coolant introduction and the combustion of H_2 fuel in an O_2 environment to minimise NOx formation, the use of H_2 as fuel increases the operating costs and releases carbon emissions when produced from fossil fuels without CCS units. Since a H_2 sales price of $\leq$ \$1.80/kg is required for a sustainable H_2 economy, the world is shifting its attention towards low-cost and low-emission sources of H_2 production [24]. The electrolysis of water (H_2O) which is considered a sustainable route for H_2 production requires integration into other thermal units to reduce the obtained H_2 sales price which ranges from \$5.10/kg_{H_2} to \$10.3/kg_{H_2} [25]. At a purchase price of \$3.89/kg_{H_2}, distilled H_2O production for H_2O electrolysis costs \$0.084/kg_{H_2} [18]. Thus, the integration of solar or wind powered electrolysis of H_2O to utilise the recovered waste heat for feedstock (distilled H_2O) production and to produce H_2 fuel and O_2 oxidant for the decomposer furnace can further reduce the operation cost and carbon emissions.

In the electrolysis of H_2O, H_2 and O_2 are produced in the cathodic and anodic chambers by the passage of electricity between 2 separated electrodes. The production of H_2 was due to the electrochemical dissociation of the H_2O molecule. This renewable method of producing both H_2 and O_2 requires DC (direct current) from solar, wind, geothermal and other renewable power sources to eliminate carbon footprints from the process. Among the three dominant types of H_2O electrolysis cells such as alkaline electrolysis cell (AEC), solid oxide electrolysis cell (SOEC) and proton exchange membrane electrolysis cell (PEMEC), fast response time, larger surface area, and low operating temperature (100 °C) are advantages of PEMEC. Considering the benefits of PEMEC, application into small-scale units can be beneficial [26].

The application of AEC and SOEC electrolysis of H_2O into biomass pyrolysis was also investigated in our earliest studies. The result showed improved efficiency in the anodic oxidation of SO_2 in AEC and cost reduction in SOEC. On the other hand, low-temperature AEC and high-temperature SOEC were investigated because of the involvement of sulphuric acid and CSP units [18]. Other related studies investigated include the use of natural gas-fired pyrolysis of municipal solid waste and H_2 produced from electrolysis to operate a fuel cell for methanol production. Lower CO_2 emission, a conversion efficiency between 44 % and 94 % and cheaper methanol sales price were recorded [27]. In addition, H_2 production from combined biochar and electrolysis of H_2O was also investigated by Ying et al. and reported improved conversion efficiency compared to hydrothermal carbonisation (HB) of rice husk [28]. The improved efficiency was attributed to the minimal resistivity to the charge transfer despite lower current density in contrast to HB. Lately, electrolysis of H_2O powered by solar energy was developed as a single unit using triple-junction solar cells. The developed unit of H_2 production with a lower cost of materials achieved 31 % peak efficiency during 48hrs testing. Nonetheless, the use of high-grade materials such as noble metals was recommended by the author to increase the efficiency. Furthermore, 95 % efficiency for a 3hrs test duration with peak solar irradiance was reported in the hybrid solar electrochemical splitting of H_2O to produce H_2. While energy storage route through the electrolysis of H_2O coupled with wind turbine systems during low demand of energy was suggested for locations with higher wind speed [29–31]. At the moment, syngas recovery from municipal plastic waste (MPW) to minimise ecological damage and the electrolysis of H_2O using

H_2 by-product as pyrolysis furnace fuel can save the ocean and promote proper plastic waste management. Eqs. (2)–(4) are chemical reactions of H_2 conducting PEMEC.

$$\text{Anode} : 2H_2O \rightarrow 4H^+ + O_2 + 4e^- \tag{2}$$

$$\text{Cathode} : 4H^+ + 4e^- \rightarrow 2H_2 \tag{3}$$

$$\text{Overall} : 2H_2O \rightarrow 2H_2 + O_2 \tag{4}$$

In summary, a greater amount of plastic waste in landfills ends up in the ocean and forms ocean-bound plastic waste (OPW). Some of the plastic waste found in the ocean came from abandoned fishing equipment. If the continuous flow of plastic waste to the sea persists, marine life will find it difficult to adapt to the new ecosystem. Fast pyrolysis was considered the best route for waste plastic management because of catalyst diffusion in the feedstock pores in catalytic pyrolysis and the low efficiency of the mechanical route. In addition, fast pyrolysis produces less liquid oil, which reduces bio-oil stability, quality and upgrade issues. The transition from fossil fuels to oxy-hydrogen combustion in the pyrolysis furnace and the use of renewable power systems such as wind and solar can eliminate carbon footprints from the process. Feeding CO_2 by-product to the pyrolyser and mixing the process CO_2 with other solid residues for soil nourishment can improve crop yields and reduce carbon emissions. The introduction of the electrolysis of H_2O to produce both H_2 and O_2 for furnace fuel and oxidant can reduce operating costs.

Therefore, this study proposed a sustainable means of MPW-to-fuel (H_2) through a fast pyrolysis system and solar or wind aided saltwater electrolysis to increase H_2 production rate and produce O_2 for the pyrolyser oxy-hydrogen furnace, which is missing in the literature. The use of CO_2 instead of N_2 as a reaction medium and the absence of process CO_2 by reacting with carbon and ash (solid residues), were investigated for soil improvement. Thermal cracking of MPW in the pyrolyser unit was considered over catalytic MPW to recover sufficient heat for saline (saltwater) desalination to feed the electrolyser system and prevent catalyst deactivation. Both solar and wind renewable power systems generate electricity for the electrical units to prevent electricity dependency on the grid. Process CO_2 capture and oxy-hydrogen combustion in the decomposer furnace to exclude carbon footprints from the process were covered. Other aspects covered in this study include an economic analysis and an environmental assessment by estimating the amount of CO_2 that will be prevented by replacing natural gas (NG) with H_2 as the pyrolysis furnace fuel. This approach will encourage the removal of plastic waste from landfills and oceans in a way that produces negative greenhouse gas (GHG) emissions and generates a profit. The below points were considered during the process development and simulation of the proposed system using Aspen Plus, Matlab-Simulink and Ansys Workbench software.

a. Process simulation of fast pyrolysis of MPW to produce gases and solid residues (carbon) with minimal liquid oil.
b. Investigation of CO_2 feed to the pyrolyser for better biochar stability and for carbon sequestration.
c. Application of heat recovery unit to operate downstream units such as saltwater desalination to feed the electrolyser stack.
d. Electricity generation from renewable solar and wind energy sources to power the electrical units.
e. PEM electrolysis of H_2O for H_2 and O_2 production.
f. Oxy-hydrogen furnace for thermal decomposition of MPW feed.
g. Utility analysis to calculate the volume of CO_2 prevented by substituting natural gas with H_2 fuel.
h. By-product CO_2 capture and reuse for soil nourishment.

Fig. 1 displays a schematic diagram of solar and wind assisted MPW pyrolysis coupled with PEMEC and CO_2 capture.
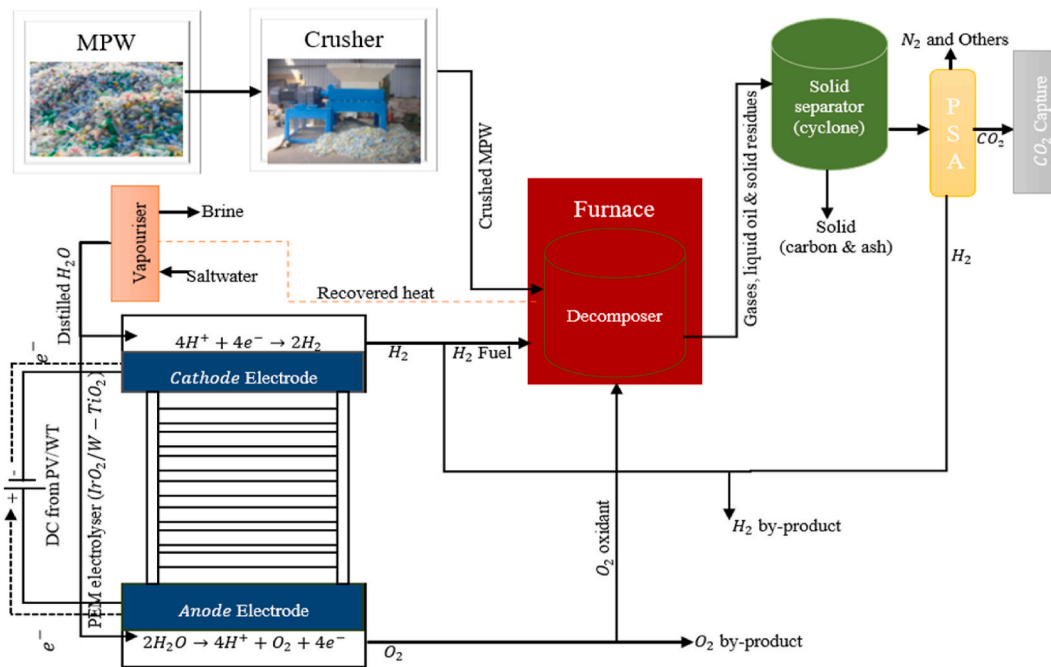
Fig. 1. Schematic diagram of solar and wind aided MPW pyrolysis coupled with PEMEC and CO_2 capture.

2. Material and simulation procedure

The feedstock considered in this proposed system was a combination of polyethylene terephthalate (PET), high-density polyethylene (HDPE), polyvinyl chlorine (PVC), low-density polyethylene (LDPE), polypropylene (PP) and polystyrene (PS). This is necessary because different types of plastic waste end up in landfills and oceans. The proximate and ultimate analyses of this simulated model are the average of PET, HDPE, PVC, LDPE, PP and PS taken from the literature as shown in Table 1. The simulated model excludes washing and drying before grinding in the crusher. However, to reduce the moisture content, natural drying or the use of N_2 gas for feedstock drying is necessary. Conventional, solid, pseudo and nonconventional component types were selected. Carbon and ash are considered solid, by-product gases are regarded as conventional, saltwater (CLH_2NaO) as a pseudo component and MPS as nonconventional. Both HCOALGEN and DCOALIGT were activated to set the proximate, ultimate and sulphur analyses because of the absence of chemical or phase equilibrium participation of nonconventional component. Equations (2)–(4) which describe the electrochemical reactions of PEMEC were registered in the property chemistry. Peng-Robinson and non-random two-liquid (NRTL) equation of states were activated to accurately simulate the thermolysis and electrochemical reaction of plastic waste and desalinated H_2O. Other considered methods for the solver were ideal gas property and steam table free

water for proper adjustment and accommodation of pressure deviation. MCINCPSD for stream class and both mixed, CIPSD and NCPSD for substreams classes in the simulation settings. MCINCPSD stands for mixed (M), conventional inert (CI), nonconventional (NC) and particle size distribution (PSD). PSD parameters set up considered logarithmic grid type with an interval of 10, 0.5 mm lower and 5 mm upper limits. Thermal and electricity for utility settings utilised natural gas as furnace fuel to estimate the amount of carbon emissions prevented by burning H_2 fuel in an O_2 environment. The rigorous reactor (RGibbs) replaced a fixed or fluidized bed pyrolysis reactor to produce sufficient heat for saltwater desalination.

2.1. Overview of renewable solar and wind power sources for electrical units of the proposed system

Matlab-Simulink software was used in the development of renewable solar and wind energy systems. The power output of the developed electrical energy units was distributed to the electrical equipment of the Aspen Plus file to have the proposed system functioning as a single unit. Eqs. (5)–(9) and Eqs. (10) and (11) written below describe the solar cell and wind turbine system for converting photon and kinetic energies to electrical energy.

$$I = I_{PV} - I_D \tag{5}$$

Table 1
Proximate and ultimate analyses of plastic waste from the literature and current study.

Ref	MPW Types	Proximate analysis (wt%)				Ultimate analysis of elements (wt%)				
		Moisture (%)	Volatile matter (%)	Fixed carbon (%)	Ash (%)	Carbon (C)	Hydrogen (H_2)	Oxygen (O_2)	Nitrogen (N)	Sulphur (S)
[32]	Polyethylene terephthalate (PET).	0.1	88.1	11.8	0	62.1	4.4	33.5	0	0
[33]	High-density polyethylene (HDPE).	0	100	0	0	80.58	13.98	5.19	0.60	0.080
[34]	Polyvinyl chlorine (PVC).	1.86	76.4	19.02	2.74	31.7	7.31	55.7	0.31	0.41
[35]	Low-density polyethylene (LDPE)	0	99.90	0.05	0.05	85.7	14.14	0.16	0	0
[36]	Polypropylene (PP).	0	99.5	0.5	0	85.56	13.85	0.59	0	0
[32]	Polystyrene (PS).	0	99.9	0.1	0	92.8	7.2	0	0	0
This study	MPW (combined PET, HDPE, PVC, LDPE, PP and PS).	0.326	93.966	5.245	0.465	73.073	10.1466	16.54708	0.15166	0.08166

$$I_D = I_0 \left[exp \frac{V}{AV_T} - 1 \right] \tag{6}$$

$$I = I_{PV} - I_0 \left[exp \frac{V}{AV_T} - 1 \right] \tag{7}$$

$$I = \left[exp \left(\frac{V + I * R_s}{I_{PV-}, 0*V_T} \right) - 1 \right] \tag{8}$$

$$P = V \left\{ I_{sc} - I_0 \left[exp \left(\frac{V}{AV_T} \right) - 1 \right] \right\} \tag{9}$$

where: I, I_{PV}, I_D, I_0 & I_{sc} are PV output current; generated current by the incident of light; bypass diode current as dependence to junction voltage; diode reverse bias saturation current; short circuit current. V, AV_T, R_s are voltage; ampere voltage climate temperature; series resistance.

$$P_w = 0.5 C_p \rho * A * V_w^3 \tag{10}$$

$$T_w = P_w W_w \tag{11}$$

where: P_w, C_p, ρ, A & V_w are power derived from a wind turbine; coefficient of performance; air density; covered area by the blade rotor. T_w & W_w are aerodynamic torque; turbine rotor speed [37,38]. Table 2 lists the input parameters considered for the development of both solar cells and wind turbine (WT) systems in Matlab-Simulink.

2.2. Assumptions and overview of pyrolysis of plastic waste for gases, solid residues and liquid oil production

The assumptions taken into consideration in the process simulation of MPW pyrolysis and PEM electrolysis of H_2O are listed below:

- Steady-state condition for all units.
- The feed operating parameters such are temperature and pressure are atmospheric and ambient.
- The operating parameters used for the process simulation were taken from the literature and sensitivity analyses.
- Thermal energy is produced in the Rigorous reactor (RGibbs) and fed to the decomposer.
- H_2 gas for furnace fuel and O_2 gas as oxidant.
- H_2 flammability is between 4 % and 75 % in air [39–41].
- 13:1 O_2 to H_2 mass ratio which is equivalent to 62:1 air to H_2 ratio.
- 1 kg of H_2 and 13 kg of O_2 releases $\geq$111 MJ/kg.
- The utility settings considered EU-2007/589/EC data source and natural gas as furnace fuel to calculate the volume of CO_2 emission.
- 0.85 for the CO_2 energy source efficient factor and 42 MJ/kg heating value for the decomposer furnace.
- 0.58 for the CO_2 energy source efficient factor and 42 MJ/kg heating value for electricity at 0.117$/MJ purchased price.
- CH_2O_2, C_6H_6O, C_2H_4O, $C_2H_4O_2$, $C_2H_2O_2$, $C_5H_{10}O_5$, $C_6H_{10}O_5$, $C_6H_6O_3$, CH_4O, $C_2H_6O_2$, CH_2O, C_3H_6O, $C_9H_{10}O_2$ and $C_{11}H_{12}O_4$ for pyrolysis liquid oil composition [42]
- The saltwater is a solution of H_2O and $NaCl$ at a mass ratio of 60:40.
- CO_2 capture by reacting with CaO.

Table 2
Design parameters for wind Turbine (WT) and solar cell (SC).

Wind turbine parameters		Solar cell parameters	
Parameters	Value	Parameters	Value
Rated power	250 kW	Rated power	250 kW
Maximum cp	0.45	Array type	Roof mount
Cut-in wind speed	4 m/s	Tilt	0°
Cut-off wind speed	25 m/s	Azimuth	180°
Total system loss	18 %	Total system loss	14 %

- Absence of deactivation during multiple desorption-reduction cycles.

In the MPW feed stream, 50 kg/h of total flowrate, NCPSD substream, ambient temperature and atmospheric pressure were the input parameters. The proximate and ultimate analyses parameters listed in Table 1 were used as the fraction value without sulphur analysis. The MPW feed standard distribution function settings considered normal type between 0.001 m and 0.005 m and the activation of PSD logarithmic mesh type. Gyratory crusher type, US bureau of mines selection and breakage functions, 0.005 m maximum particle diameter and cut-off side to solid outlet diameter of 1.7 ratio were selected for the MPW feed crusher. Electricity and thermal ID were activated for the utilities. A nonstoichiometric reaction (Ryield) based on known yield distribution was utilised to decompose MPW into carbon, H_2, O_2, N_2, sulphur and ash as components and ultimate analysis fraction illustrated in Table 1. A rigorous reactor (RGibbs) was used to produce gas, char, ash and liquid oil at 10 bar pressure and 800 °C temperature by activating carbon, H_2, CO_2, N_2, methane (CH_4), sulphur, ash and others (liquid oil) in the component section. In the solid separator (cyclone), a fraction of 1 for non-mixed and 0 for mixed substream were adopted. While a PSA unit consisting of different columns separates syngas from other gases based on specified fractional values for all elements. A rigorous reactor (RGibbs) was also used to react CaO with CO_2 by-product to form $CaCO_3$ for storage at a suitable location and to mix process CO_2 with other solid residues for soil nourishment. Distilled H_2O production by using heat exchangers to cool the decomposer by-products. In heat exchangers, saltwater as a cold stream and pyrolysis decomposer by-product as a hot stream produced deionised H_2O feed to the electrolysis stack.

In addition, the decomposer furnace considered a rigorous reactor (RGibbs) with H_2 as fuel and O_2 as an oxidant to release the thermal energy necessary to reach the reaction temperature and heat duty. The numerical model for H_2 combustion and the decomposition of MPW were further investigated in Ansys Workbench. Three-dimensional (3-D) equilibrium Navier-Stokes equations and a feasible (realisable) standard wall functions k-ε model for the H_2 furnace and an Euler-Euler multiphase solid and gas phases were utilised. As shown in Eqs. (12)–(17), the conservation of energy, momentum, species transport and thermal nitric oxide (*NO*) equations for the combustion of H_2 and individual solid and gas phases were solved.

$$\frac{\partial}{\partial t} + \frac{\partial}{\partial x_i}(\rho u_i) = 0 \; (Continuity). \tag{12}$$

$$\frac{\partial}{\partial t}(\rho u_i) + \frac{\partial}{\partial x_i}(\rho u_i u_j - \tau_{ij}) = \frac{\partial_p}{\partial x_i} \; (Momentum). \tag{13}$$

$$\frac{\partial}{\partial t}(\rho u_j) + \frac{\partial}{\partial x_i}(\rho h u_j) = \frac{\partial(\lambda_f \partial T_f)}{\partial x_i} - \sum_j \frac{\partial(h_j J_j)}{\partial x_i} + \sum_j h_j R_j \; (Energy) \tag{14}$$

$$\frac{\partial}{\partial t}(\rho_s c_s T_s) + \frac{\partial}{\partial x_i}\left[\lambda_s \frac{\partial T_s}{\partial x_i} \right] = 0 \; (Energy) \tag{15}$$

$$\frac{\partial(\rho Y_i)}{\partial t} + \frac{\partial(\rho u_i Y_i)}{\partial x_i} = \frac{\partial J_i}{\partial x_i} + R_i \; (Species) \tag{16}$$

$$W_t = \left[4.5 \frac{[10^{13.5} * m^{1.5}]}{mol^{0.5}.s} \right] exp \left[\frac{-69466K}{T} \right] c_{O_2}^{0.5} c_{N_2} \left(\frac{T}{1K} \right)^{-0.5} \; (Thermal \; NO) \tag{17}$$

where: ρ = fuel (H_2) density; u = velocity; τ_{ij} = stress tensor; h = enthalpy; J_i = species i heat capacity; T = temperature; R_j = net rate for species j chemical reaction; Y_i = mass fraction of species i; λ = thermal conductivity; f = working fluid; s = solid wall; c_{N_2} = nitrogen molar concentration; p = pressure.

PEMEC for H_2 and O_2 production. In the electrochemical reaction of deionised H_2O feed, a Gibbs reactor block with PEMEC chemical re-

actions described in equations (2)–(4) was implemented to produce both H_2 and O_2 in a ratio of 2:1. Electricity instead of heat input was also considered during the PEMEC stack settings. Aspen Plus blocks and material streams with descriptions are listed in Table 3.

2.3 Development of solar and wind power systems for electrical units of the proposed system.

As shown in Fig. 2 (combined solar and wind renewable energy system), a solar energy system converts photon energy to electrical energy when the irradiance of the sun reflects on the photovoltaic (PV) arrays. PV cells usually have p-type and n-type semiconductor materials that release and accept electrons due to temperature differences. This movement of electrons from p-type to n-type generates electricity. The voltage and current of the developed solar system were measured by both voltage and current measurement blocks. Whereas the multiplier (product block) estimates the total power output of the solar system which is 25 kW. Similar to the solar energy system, the wind turbine system generated 25 kW power output by converting mechanical to electrical energy. The capacity of individual electrical systems was increased to 250 kW.

Table 3
List of Aspen Plus unit operation model blocks and material streams descriptions.

Aspen Plus Block Name	Aspen Plus Block ID	Description
Mixer	H_2 MIXER	Mixed H_2 from PSA and PEMEC. Merge 2 streams.
Hierarchy	DECOM/PEMEC	Container for directories. Act as a subsystem having a set of blocks that are grouped into a single hierarchy block. House RGibbs for the decomposition of crushed plastic waste feed and the electrochemical dissociation of saltwater into H_2 and O_2.
Rigorous reactor (RGibbs)	COMB/CO_2-CAPT/H_2-COMB/C-CO_2-R	Set the composition of product/syngas by chemical equilibrium restriction. Gibbs free energy reactor. To produce liquid oil, gases and solid residues. For CO_2 capture. For heat production by combusting H_2 in an O_2 environment.
Heater	COOLER	Thermal and phase state changer. For cooling desalinated H_2O feed to the electrolysis stack
Heat exchanger	HX/COM	Transfers heat from one medium to another. For waste heat recovery. To produce deionised H_2O from saline.
Splitter	H_2- FLO-C/O_2- FLO-C	Divide feed based on splits specification for the outlet streams. For H_2 and O_2 flow control to the H_2 furnaces.
Separator	PSA/STEAM-GE	Split/separate products based on specified flows/fractions. Separate H_2 gas from others. Separate distilled H_2O from brine.
Solid separator	CYCLONE/S-SEP	For separating solids from gases or liquids based on specified fractions. For separating carbon (char) from ash.
Pump	STEAM-PU	Increase feed pressure to the desired level. More effective in the liquid phase.
Crusher	CRUSHER	To reduce the size of solid particles.
Aspen Plus stream ID		Description
MPW-FE		Municipal plastic waste feed.
DECO-MPW		Decomposed municipal plastic waste feed.
HEAT-MPW		Heated municipal plastic waste feed to the pyrolysis reactor.
S-H_2O		Saltwater or saline.
DIS-H_2O		Distilled H_2O.
SYN		Synthetic gas or syngas.
CO2C-ASH		Mixture of solid residues (carbon, ash and CO_2).
BY-H_2/H_2-BY/any stream with H_2		H_2 by-product.
BY-O_2/O_2-BY/any stream with O_2		O_2 by-product.

2.3. Process development of an integrated pyrolysis of MPW and PEMEC in Aspen Plus

In the simulated model displayed in Fig. 3a, MPW is fed to the crusher to reduce the particle size to < 5 mm prior to the first decomposer. In the upstream devolatilisation zone, the yield fraction of the exit product was specified based on the ultimate analysis before entering the final decomposer. Devolatilised feed was heated to a temperature of 800 °C to produce gases, liquid oil and solid residues such as carbon (C), H_2, CO_2, N_2, CH_4, sulphur (S), ash and others. The cyclone allowed the solid to settle at the bed leaving the gases at the top before cooling in the heat exchanger with pressurised saltwater. Carbon was separated from the ash and stored, while H_2 was recovered from other gases in the PSA column. Recovered thermal energy from both solid and gas cooling was used to produce distilled H_2O feed to the PEMEC stack. Cooled deionised H_2O from the cooler was dissociated into H_2 and O_2 with the applied voltage < 1 V. H_2 from the electrolyser stack and PSA unit mixes prior to the splitter where 1.55 kg/hr_{H_2} combusted with 20.15 kg/hr_{O_2} in the decomposer furnace. Further 1.155 kg/hr_{H_2} and 14.3 55 kg/hr_{O_2} from both splitters were combusted in the second H_2 furnace to make up losses in the heat exchangers. The flow volume of both H_2 and O_2 to the combustors were controlled in H_2 and O_2 splitters. To remove carbon emission footprints from the process, CaO was utilised to absorb CO_2 for transportation to a storage location. The absorption method of CO_2 capture at ambient temperature and atmospheric pressure conditions was exothermic, unlike other thermal units. Since the production of thermal energy was performed in different combustors (furnaces), the heat stream was connected to the MPW decomposer. The heat stream from the second H_2 furnace (H_2-COMB2) can be linked to other thermal units to meet the reaction temperatures and heat duties. For the simulated integrated pyrolysis and electrolysis of H_2O system shown in Fig. 3b, the CO_2 capture unit was excluded to allow the feeding of process CO_2 to the pyrolyser and mixing with other solid residues such as char and ash for soil nourishment. Contaminated soils' improvement and increase in crop yields by adding char mixed with CO_2 have been promoted to reduce the impact of climate change caused by the continuous GHG emissions.

2.4. Numerical study of oxy-hydrogen combustion in the fluidized bed reactor (FBR) furnace for MPW decomposition

Mesh independency was checked using face, sizing and refinement meshing types. For the numerical study of an integrated H_2 furnace and FBR, an element number of 952,799 cells was adopted as nearly the same result was seen by increasing the cell numbers. For instance, $> 10^{-6}$ energy equation and other convergence criterion equations were reached at an element number of 952,799 cells. Fuel and air mass flowrate, and feedstock velocity magnitude inlets, exhaust gas and syngas pressure outlets and reflective non-slip walls were the boundary conditions for the hybrid H_2 furnace and FBR unit. Lean-burn H_2 in a furnace at ambient temperature and atmospheric pressure and a MPW (combination of PET, HDPE, PVC, LDPE, PP and PS) density of 1093.6633 kg/m^3 were utilised. In this sub-section of this work, the mass flowrate of MPW to the FBR and by-product syngas and solid were not considered because the pyrolysis decomposition of MPW is already studied in Fig. 3a. However, an inlet velocity magnitude of 0.31 m/s was used. The solid secondary phase for the MPW considered a granular type with a 0.00028 mm diameter and syamlal-obrien viscosity in the Euler multiphase solid and gas phases. Although, the syamlal-obrien parameter was utilised as a drag coefficient in the force Euler multiphase settings. The second-order implicit transient formulation for the solution method and 0.4 vol fraction for the solid phase patch were set for the syngas exit to the cyclone solid separator as described in Fig. 3a. The combined H_2 furnace and FBR are displayed in Fig. 4.
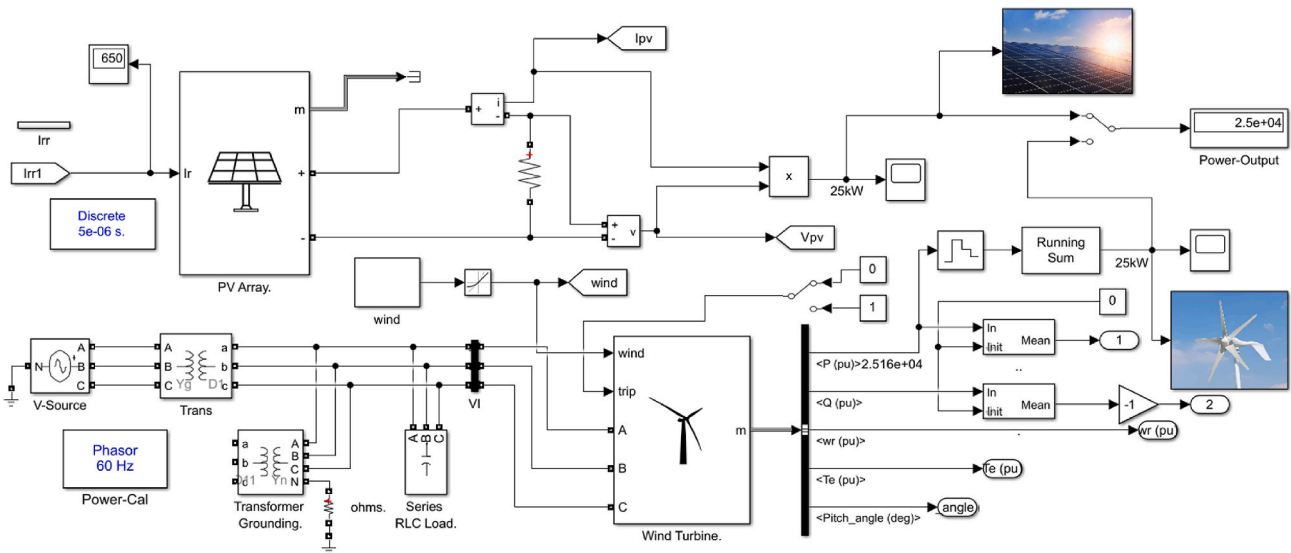
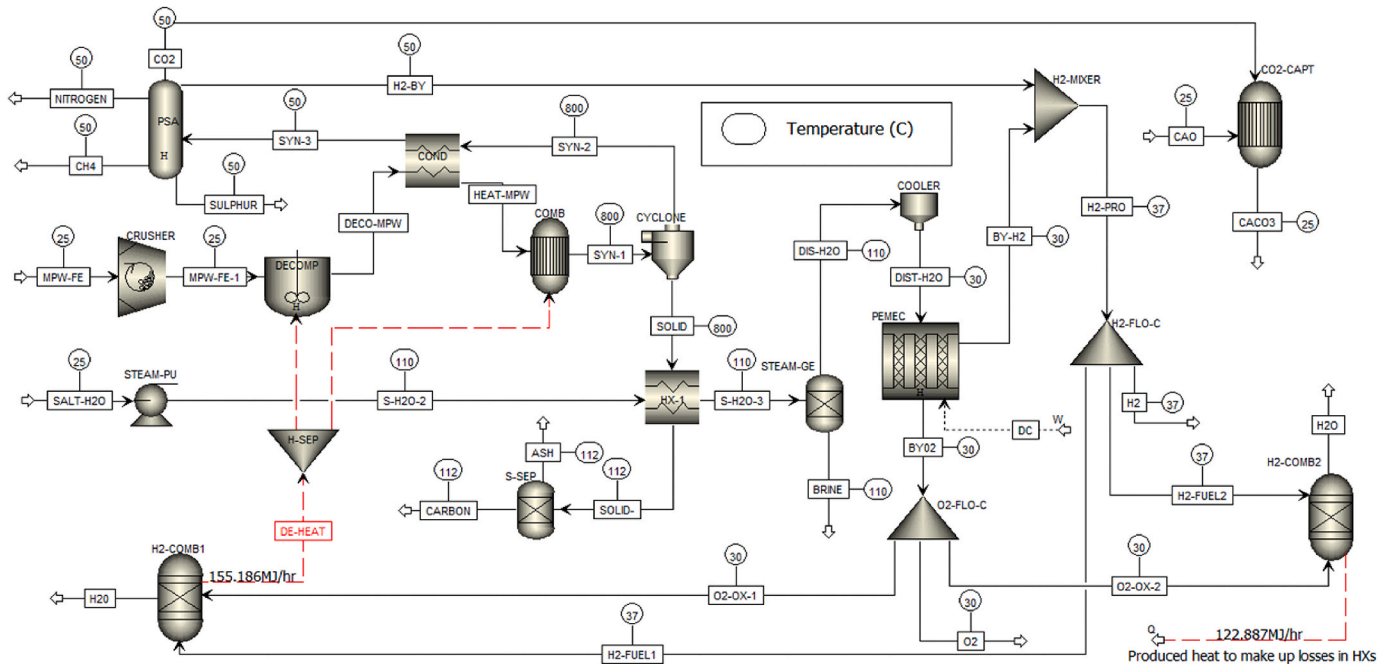**Fig. 2.** Matlab-Simulink of hybrid solar and wind power systems.

Fig. 3a. ASPEN Plus flow diagram for pyrolysis of MPW coupled with PEMEC and CO_2 capture.

2.5. Solar or wind assisted pyrolysis MPW and electrolysis of saltwater as an integrated system

To connect the generated electricity by the developed solar PV or wind turbine systems to the simulated Aspen Plus model such as the electrolyser stack, the model was transformed into flow-driven and exported to the Simulink. This is necessary because Aspen Plus is limited to the development of both renewable solar and wind power systems. In the hybrid system as shown in Fig. 5, a power switch was introduced for energy management. The electricity generated from either wind or solar system was connected to the electrolyser stack and some other electrical units to have the proposed system operate as a single unit. The flexibility of power distribution to other electrical units is possible to achieve net-zero H_2, O_2 and carbon production in ocean and landfill plastic waste recycling and management.

3. Results and discussions

The developed model achieved high gas production because of high heating temperature and the use of MPW feedstock of < 5 mm particle size. This is necessary to reduce the yield of solid residues and liquid oil as Luo et al. reported low syngas yield because of incomplete decomposition of larger feedstock particle size [43]. Smaller feed particle sizes are unfavourable to char and liquid oil production because of a faster heating rate. O_2 was present in the ultimate analysis but was missing in the final product. The absence of O_2 in the final gas composition was attributed to the formation of CO_2 by-product. The application of fast thermal pyrolysis instead of slow catalytic pyrolysis paved the way to produce distilled H_2O from seawater, reducing the operation cost of ocean cleanup. Using H_2 as fuel without catalysts in the decomposer, the proposed system can accommodate a mixture of MPW and biomass without considering the effect on catalyst recovery. CO_2 emission was
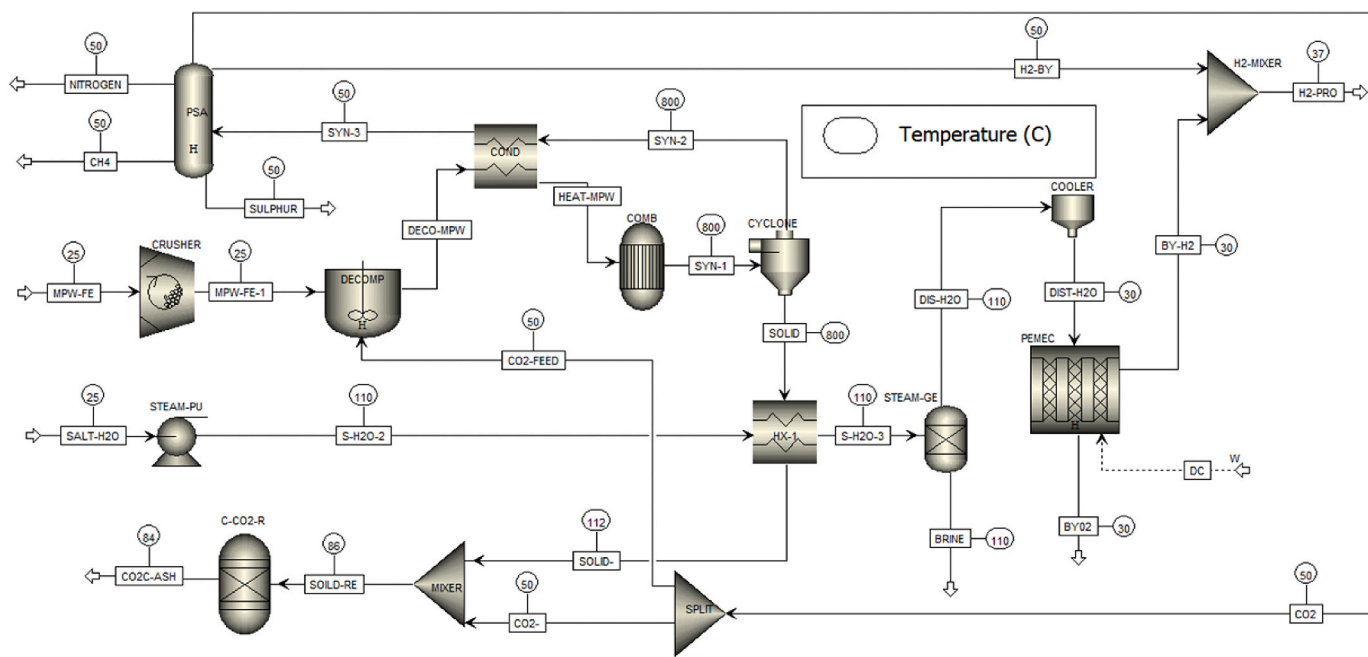
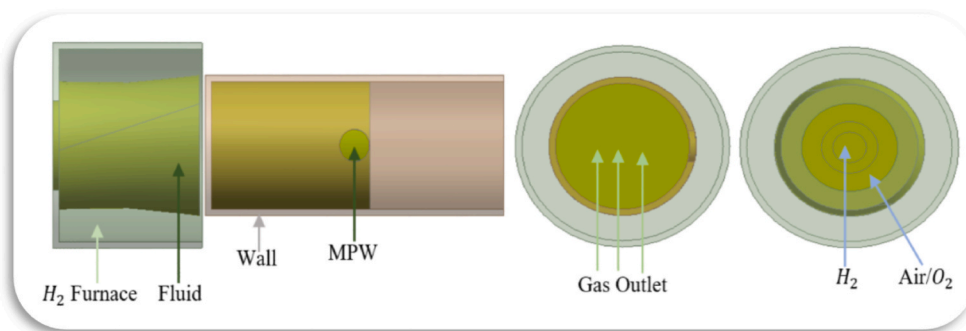**Fig. 3b.** ASPEN Plus flow diagram for pyrolysis of MPW coupled with PEMEC for carbon sequestration.

Fig. 4. H_2 furnace and fluidized bed reactor (FBR).

removed from the process by burning H_2 fuel and reacting CaO with the by-product CO_2. H_2 yield of fast pyrolysis was relatively small compared to carbon (C) which accounts for 56 % of the total by-product. The introduction of a PEM electrolysis cell with an input power of 241.2 kW increased the H_2 by-product of the integrated system. 2.65 kg/h of H_2 fuel, which is 29 % of the total production, was enough to reach the operating decomposer temperature and heat duty. Similar to H_2 fuel, 34.45 kg/h of O_2 oxidant was also utilised in the decomposer furnace. 34.45 kg/h of O_2 oxidant accounts for 71.8 % of the total production. This result shows that an increase in MPW feed >17 % requires an increase in saltwater feed to produce more O_2 oxidant to the decomposer furnace. The capture of CO_2 (11.3 kg/h) by-product released 45.895 MJ/h of heat which can be recovered to produce more distilled H_2O feed to the electrolyser stack. While 25.68 kg/h $CaCO_3$ was formed during the exothermic capture of the CO_2 by-product. A small fraction of produced H_2 fuel can be burnt to release CO_2 from CaO during underground storage.

In the hybrid pyrolysis and electrolysis system with CO_2 feed to the pyrolyser to enhance the stability of both liquid oil and biochar, an increase in energy input by 11 % was observed, while the formation of CO (0.5 kg/h) was also noticed. Table 4 reports the simulated result of the proposed system. Heat and electricity inputs to thermal and electrical units and CO_2 avoided by substituting natural gas with H_2 as the furnace fuel are reported in Table 5. The electricity input to the PSA and other

separation columns was excluded from Table 5 because of the relatively small values of brake power/heat duty. However, Kohlheb et al. mentioned that between 0.2 and 0.34 kWh/Nm^3 biogas electrical power is needed to operate the PSA column [44]. In addition, PSA for H_2 recovery requires 2.4 kW/kg for operation. PSA of a fast pyrolysis unit requires 7.7 kW electricity and releases 2.6 kg of CO_2 when the electricity is generated from the natural gas powerplant.

For the solar power and wind turbine systems, an increase in power outputs as the irradiance and wind speed increased were observed. These show that higher irradiance (<1000 W/m^2) at ambient temperature conditions and wind speed of <17 m/s influences the power output of solar PV and wind turbine energy systems. A factor of 8 increments of wind energy power output was seen by doubling the wind speed without increasing the size of the blades. Furthermore, the power of the wind turbine can also be enhanced by increasing the length of the blades to extract more kinetic energy from the wind. By using Eq. (18) which is an equation for estimating the efficiency of the system, ≥70 % efficiency was recorded. The estimated efficiency is the average efficiency of both pyrolysis and electrolyser units.

$$Efficiency\ (n) = \frac{(H_2\ LHV * mass\ flowrate\ of\ produced\ H_2) + (CH_4\ LHV * mass\ flowrate\ of\ produced\ CH_4)}{Energy\ input} \tag{18}$$
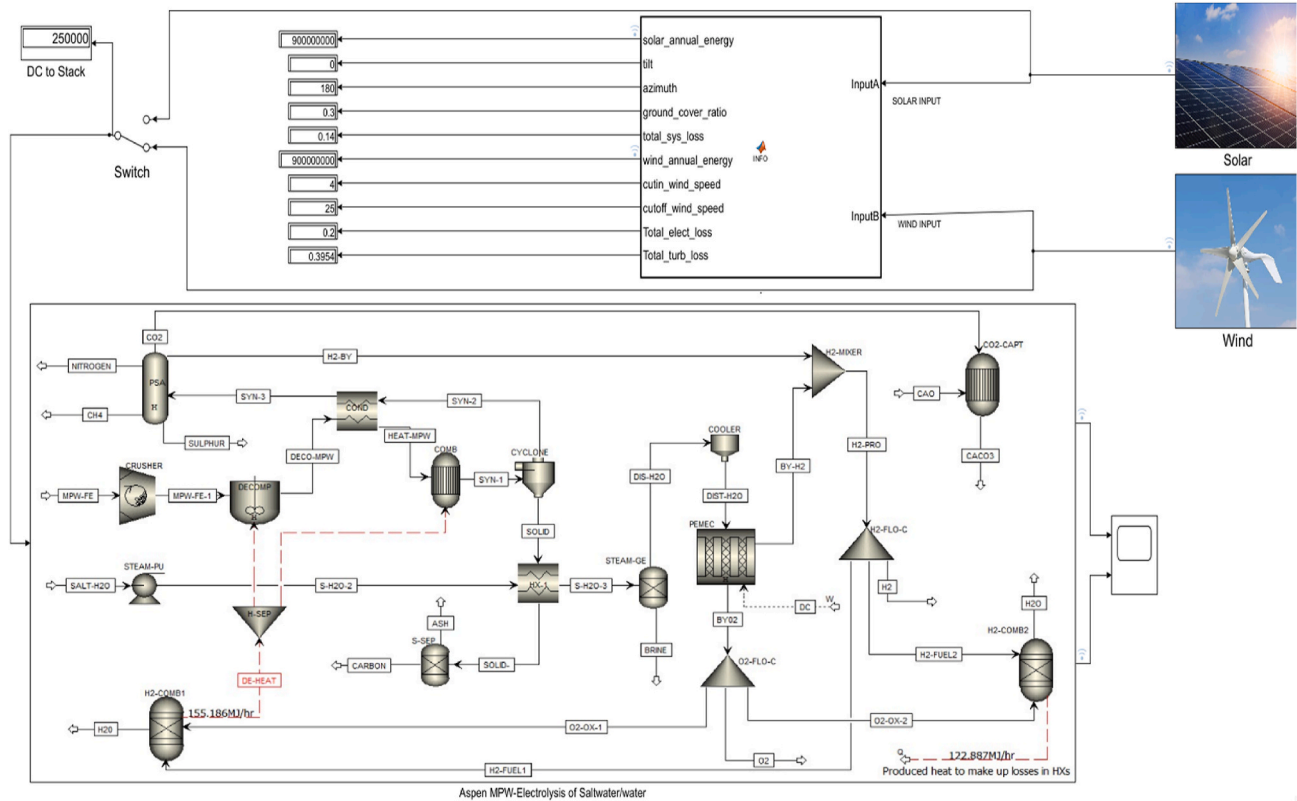

Fig. 5. Solar and wind aided pyrolysis of MPW coupled with PEMEC and CO_2 capture.

Table 4
Feed and product results of integrated pyrolysis of MPW coupled with PEMEC processes for H_2 production.

Unit	Feed (kg/hr)				Product (kg/hr)										
	MPW	Saltwater	H_2O	CaO	C	H_2	O_2	CO_2	CH_4	H_2O	N_2	S	Ash	Oil	NaCl
Pyrolysis	50			3.7	27.7	3.2		11.3	7.4		0.1	0.1	0.24	≤0.1	
Desalination		206.97								54					153
PEMEC			54			6.04	47.9								
Total						9.24									

Table 5
Required input energies for individual units, carbon dioxide emission, biofuel and oxidant for the proposed system.

Units	Thermal energy (MJ/hr)	Electrical energy Watts (kW)	CO_2 emission (kg/hr) with NG	Required H_2 fuel (kg/hr)	Required O_2 oxidant (kg/hr)
Decomposer	155.19		10.24	1.55	20.15
Others and Heat exchanges (HE)	122.9		8.2	1.1	14.3
PEMEC stack		241.2	84		
Pressure changer		1.8	0.6		
Gas separator/PSA		Not applicable	Not applicable		
Total	278.09	243	103.04	2.65	34.45

3.1. Effect of feedstock particle size and decomposer operating temperature and pressure on by-product yields

Feedstock particle size is considered as another means of pretreatment because lower feed size favours syngas production. In this study, feed particle size with a lower limit of 0.5 mm and an upper limit of 5 mm was used to maximise the thermal efficiency of the pyrolysis unit. Syngas yield was found to increase with a feed particle size of 0.5 mm, while char production decreased. Particle size reduction is favourable for synthetic gas and liquid oil yields. Nearly the same result was reported by Hasan et al. [45]. In biological methods of syngas production such as anaerobic digestion (AD) or anaerobic fermentation (AF), smaller substrate size favours biogas yield because of higher feed degradation by microorganisms [46].

The rate at which MPW decomposed into gas, solid residues, and liquid oil is influenced by the operating temperature, residence time and pressure. In the thermolysis of biomass or plastic waste pyrolysis, the higher operating temperature of the decomposer favours gas yield because of the endothermicity of the devolatilisation. In this study, the sensitivity analyses considered reaction temperature from 50 °C to 800 °C and pressure between 1 and 10 bar. At a lower residence time and operating temperature of the decomposer, the conversion of the feedstock shifted to liquid oil. The yield of gas and solid increased as the decomposer temperature rose above 225 °C, which reduced the formation of liquid oil. The increase in gas production with increasing temperature and residence time was due to β-scission of polymer chains and homolytic dissociation of the feed (MPW). A similar result was reported by Park et al. during the study of waste polyethylene using a 2-stage pyrolyser system [47]. However, at a reaction temperature of 642 °C, the formation of CO_2 dropped for a few seconds before reaching a stable peak as the temperature increased. Unlike the increase in gas and solid yields as the reaction temperature rises, the yield of both by-products (gas and carbon) reduces as the pyrolyser pressure increases. An increase in pressure was found to promote liquid oil production, including tar formation. Nonetheless, an increase in decomposer temperature which increases the furnace fuel mass flowrate, also favours CH_4 and CO_2 productions. The effect of temperature and pressure on syngas yield in waste plastic and biomass pyrolysis follows the same trend with hydrocarbon reforming processes. For example, Shehzad et al. reported a similar result on the effect of both temperature and pressure on syngas production [48]. For this reason, both the operating temperature and pressure were kept at 800 °C and 10 bar to improve the conversion efficiency and syngas purity of the developed system. The effect of temperature and pressure on carbon and syngas production is displayed in Fig. 6a. While the profile of MPW feed devolatilisation in the FBR operating with the oxy-hydrogen furnace and thermal nitric oxide (NO) formation is shown in Fig. 6b. Thermal NOx formation is unlikely to occur due to lower operating temperature of the fast pyrolysis unit. For instance, thermal NOx formation occurs at a reaction temperature >1500 °C [49]. However, the maximum thermal NO produced from the oxy-hydrogen furnace of the FBR was $0.000036 kg/mol/m^3s$ which is < 0.1 ppm.

3.2. Effect of the reaction medium on biochar and liquid oil production

Carbon and liquid oil production were investigated to determine the effects of both CO_2 and N_2 as reaction mediums in the fast pyrolysis of plastic waste operating without a carbon capture unit. The yield of carbon and liquid oil decreases as the pyrolysis temperature increases, releasing more volatiles. The yield of both char and liquid oil was unaffected by the reaction medium (CO_2 and N_2). Nonetheless, char production and weight loss under CO_2 as an inert reaction medium was higher in contrast to N_2. The effect of weight loss as pyrolyser temperature rises was not investigated, as this study used an average of different plastic wastes to investigate the environmental and economic benefits of renewable-power-assisted hybrid pyrolysis of MPW and electrolysis of saltwater. Nevertheless, Hasan et al. confirmed that PET, HDPE, PVC, LDPE, PP and PS exhibit almost the same weight loss with increasing pyrolyser temperature [45]. Other advantages of using CO_2 as a reaction medium include the reaction with carbon to produce carbon monoxide (CO) and the reduction of fast volatilisation. The results of this investigation confirm that the surface property of the char can be affected by the reaction medium. Similar findings were reported in the literature [20,21,50]. In reference to the above literature, mixing liquid oil from biomass or municipal waste pyrolysis with low viscosity and combustible (flammable) oil such as kerosene can improve its stability. However, this study avoids the use of kerosene to store the produced liquid oil, as its (liquid oil) concentration in the end-product was very low.
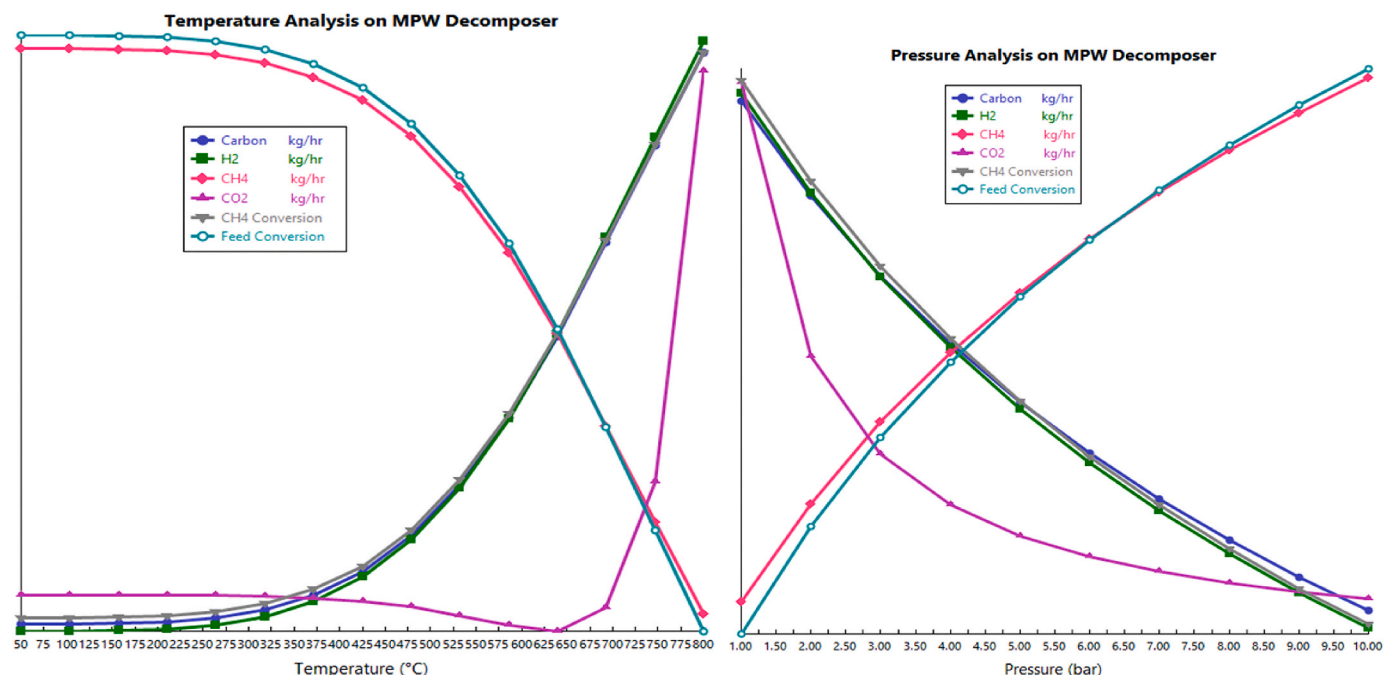

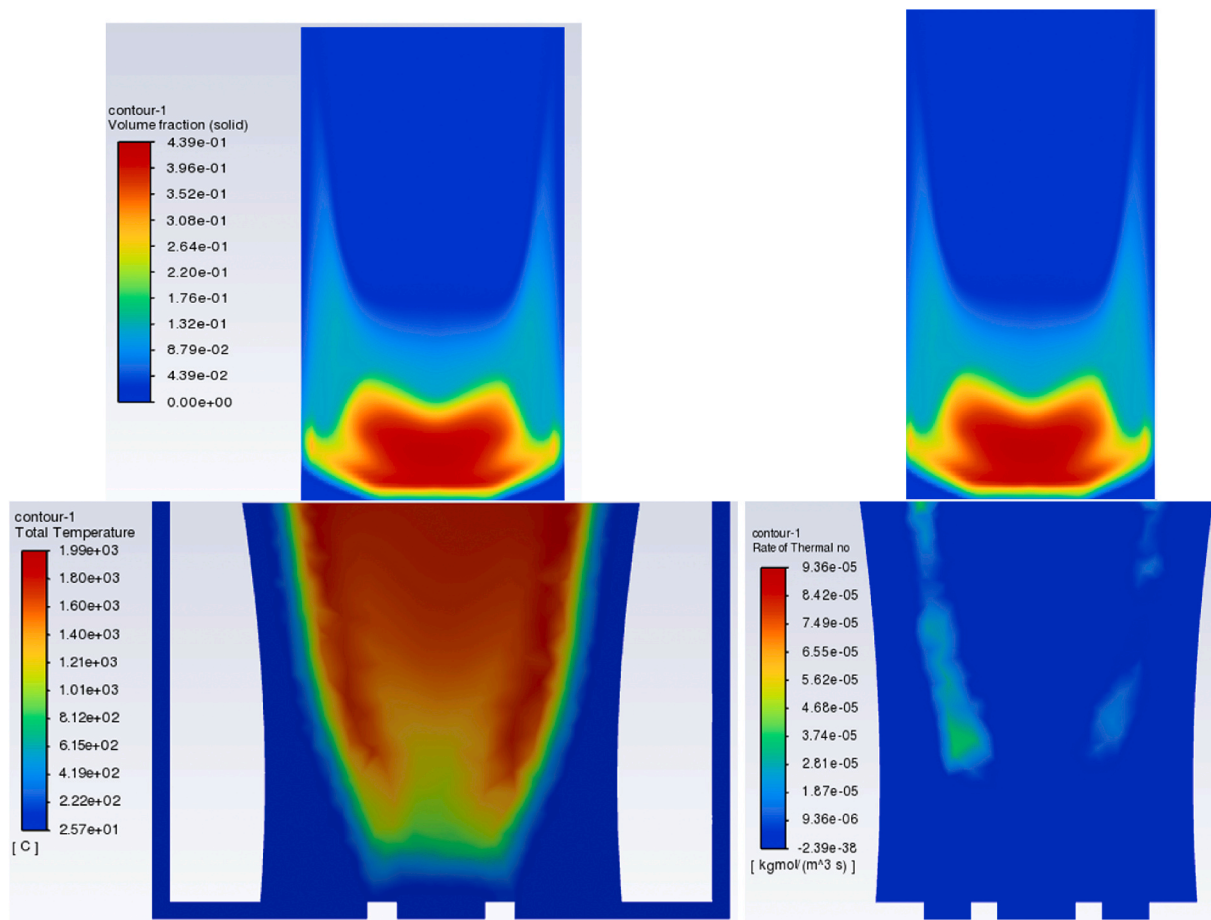**Fig. 6a.** Temperature and pressure effect on carbon and syngas yield.

Fig. 6b. MPW feed devolatilisation in the FBR operating with the oxy-hydrogen furnace and thermal NOx formation.

3.3. Model validation and comparison

The syngas and carbon yield of this simulated model were validated with the previous and related studies to understand the effectiveness of the result at a pilot-scale development. The comparison is channelled to by-products syngas and char since low liquid oil is produced and the efficiency of each unit of the hybrid system. The low yield of liquid oil including tar was attributed to the higher operating temperature and the use of H_2 as furnace fuel. During the process simulation, an increase in the conversion of liquid oil to gases and solid (carbon) was observed as reported in the sensitivity analyses above. For instance, the absence of liquid oil was reported from the investigated pyrolysis of camel manure at a reaction temperature of 900 °C [51]. In addition, liquid oil below 11 % was also reported from the pyrolysis of LDPE and HDPE at 600 °C

decomposer temperature [52]. Comparing the thermal efficiency of the pyrolysis unit of this study with that of biomass efficiency, both are in agreement. For example, pyrolysis efficiency between 45.46 % and 75.41 % and H_2 sales price of $1.77 - $2.4/$kg_{H_2}$ were reported in the literature [53–55]. Contrasting the efficiency of the pyrolysis system and the H_2 sales price of this study with the literature-reported data for solid fuel gasification, marginal differences were reached. For instance, efficiency between 43 % and 60 % and H_2 purchase price from $0.9 - $2.11/$kg_{H_2}$ for coal gasification were reported [56,57]. Although, an efficiency of $\geq$58 % and H_2 sales price $<2/kg_{H_2}$ were also reported for CH_4 pyrolysis operating with CCS unit [18,55].

Table 6 reports the validation of this study against related studies in the literature. In reference to the validation result data, carbon and gas yield in this study is slightly higher than that reported in the earlier

Table 6
Model validation on pyrolysis of plastic waste by-products and efficiency of individual units.

Ref	Feedstock	Operating temperature (°C)	Pyrolysis by-products		
			Carbon (%)	Liquid oil (%)	Gas (%)
[52]	LDPE	300–600	45–61	12–9	43–30
[61]	HDPE	500	Not reported	54.5	20.7
[52]	LDPE and HDPE	300–600	46–62.3	11–6	42–32
[51]	Camel manure	300–900	22.5		
This study	PET + HDPE + PVC + LDPE + PP + PS	800	55.9–56	<0.1	44–44.4

Ref	Units	Efficiency (%)	H_2 sales price
[53–55]	Biomass pyrolysis	45.46–75.41	$1.77–$2.4/kg_{H_2}
[56,57]	Coal gasification	43–60	$0.9–$2.11/kg_{H_2}
[18,55]	CH_4 pyrolysis operating with CCS unit	$\geq$58	$<2/kg_{H_2}$
This study	Pyrolysis of MPW and PEM electrolysis	$\geq$70	$<3.89/kg_{H_2}$

studies. Other reasons why liquid oil achieved the lowest yield (performance) can be related to the use of process simulation software, which is limited to the physical properties of plastic waste and the lack of literature data on the pyrolysis of PET, HDPE, PVC, LDPE, PP and PS mixture. Nevertheless, this study achieved a higher MPW conversion rate and energy efficiency compared to the reported data in the below Table. In contrast to SOEC, which has almost 100 % efficiency at higher reaction temperatures, and AEC, with 59 %–70 % efficiency, Sapountzi et al. [58] noted that a PEMEC efficiency ranges from 65 % to 82 %. Comparing the efficiency of PEMEC reported in the literature with the PEMEC unit in this study, a minimal difference was observed. For example, this study achieved a PEMEC efficiency of $\geq$82 %. For both wind and solar energy power systems, efficiencies of $\leq$45 % and $\leq$20 % were recorded. Similar efficiencies for both solar and wind energy systems were recorded by Ozgener and Maghami et al. during performance optimisation and investigation of power loss due to soiling [59,60].

3.4. Environmental assessment

The volume of unrecycled plastic waste that ends up in landfills and oceans due to inefficient mechanical methods has increased. In 2016, only 7 % of plastic waste was recycled in Singapore. Thus, a thermodynamic route to recover liquid oil, syngas and solid residues like carbon from plastic waste can offer cost and environmental benefits [62]. However, the pyrolysis and gasification of plastic waste to energy or fuel emits more CO_2 than the mechanical route. For instance, *Khoo*. reported 24,600 $tonnes_{CO_2}$ from mechanical, 20,200 $tonnes_{CO_2}$ from pyrolysis and 675,650 $tonnes_{CO_2}$ from other waste-to-energy routes [62]. Over the years, the growth of pyrolysis, gasification and mechanical methods of plastic waste recycling rather than other waste-to-energy routes has reduced CO_2 emission by 8 % annually. Nonetheless, further reduction of GHG emissions from waste-to-energy plants is possible by replacing fossil fuel pyrolyser and gasification furnaces with oxy-hydrogen burners. In addition, the developed system showed the feasibility of reusing and capturing by-product CO_2 to improve agricultural products. Instead of using grid electricity which can be generated from fossil fuel power stations to operate the electrical units of the developed system, green electricity from either solar or wind systems was utilised which is harmless to the environment. Thus, this proposed study provides a sustainable route to recycle and manage plastic waste without endangering the ecosystem and the environment.

3.5. Economic analysis

The proposed system is expected to achieve $\geq$70 % energy efficiency and a H_2 sales price of $< \$3.89/kg$ because of higher syngas and carbon yields. Since carbon has the largest share of the pyrolysis by-product, the purchase price of the produced H_2 is expected to reduce further if char is unused for soil improvement. For example, between \$5.10/kg and \$10.3/kg is the sales price of H_2 obtained from the electrolysis of H_2O. While \$1.50/kg is the purchase price of H_2 from fast pyrolysis of biomass without oxy-hydrogen furnaces or CCS unit. In addition, biomass carbon costs $\leq$ \$10/kg, while saltwater desalination costs more than \$0.084/kg_{H_2} at a sales price of \$3.89/kg_{H_2} [18,63,64]. In the short term, a return on investment and profit boom is expected because wind or sun, plastic waste from landfills and oceans and seawater are major sources of energy and feedstocks for the developed system. For instance, with a plant capacity of 10,000 tonnes of MPW feed per year, Hasan et al. reported a capital cost of \$2.25 million, an annual operating cost of \$775,000 and a payback period of <2 years depending on plant location [45]. A summary of both the capital and operating costs of this developed system is given in Table 7. The estimation considered a plant size of 60 tonnes per year with an average feed rate of 50 kg/h. The evaluated costs in the table below can be further reduced by increasing the capacity of the plant to accommodate more feed. By expanding the developed plant to accommodate 10,000 tonnes of MPW feed per year, the cost of pyrolysis

Table 7

Estimated capital and operation costs for the developed hybrid system.

Capital cost		Operating cost per annual	
Item	Cost (\$)	Item	Cost (\$)
Pyrolysis equipment	25,000	Feedstock sorting	18,150
Pyrolysis materials	8333.3	Labour (Depending on location)	2500–25,000
Pyrolysis installation	4166.67	Maintenance	3083–5000
PEMEC (\$1100/kW)	275,000		
Solar PV (\$628/kW)	157,000		
Wind turbine (\$1325/ kW)	331,250		

equipment, materials and installation will be reduced by 200 %–300 % using the same labour force.

As a fewer resource is required to sort the MPW feedstock, the biomass feedstock can be blended to improve the gas quality as MPW cannot be efficiently processed. The proposed innovative system recommends the use of a wind turbine system to operate the electrical units when installed in European countries like the UK, and solar power systems in countries with more sunshine. For example, an increase in wind turbine units to generate more electricity in the UK remains the best way to meet the 2050 carbon emission target [65]. Below points are some of the advantages of this developed system.

1) Carbon negative and production of distilled H_2O electrolyser feed from saltwater at the site of operation.
2) Process CO_2 and solid residues for soil improvement.
3) Electrical units powered by renewable power sources and oxy-hydrogen burners for thermal units.
4) High energy conversion efficiency and lower cost of H_2.
5) A small-scale application and an opportunity for a profitable investment that benefits the environment and the ecosystem.

4. Conclusion

Fast pyrolysis of plastic waste coupled with PEMEC and CO_2 capture and reuse for soil improvement were developed to substitute the current waste-to-energy and mechanical routes. With an $O_2 - H_2$ mass ratio of 13:1, higher gas and carbon yields without carbon emissions were achieved in the pyrolyser furnace. 29 % of produced H_2 from both fast pyrolysis and PEM electrolysis of H_2O units was consumed in oxy-hydrogen furnaces. PEMEC was used to produce more H_2 and O_2 for oxy-hydrogen pyrolyser furnaces. Carbon content of the fast pyrolysis by-product was 56 % and a reduction in H_2 sales price is expected when carbon and other valuable by-products are sold. The use of process CO_2 as a reaction medium and soil nourishment excludes the need for a CO_2 capture unit, which increases the operating costs. By using by-product CO_2 in addition to carbon and ash for soil nourishment, a minimal reduction in H_2 sales price is expected. The developed system achieved $< 0.136 kg/mol/m^3s$ thermal NO, $\geq$70 % energy efficiency of the pyrolysis and electrolysis units and $< \$3.89/kg_{H_2}$ sales price. Solar and wind power systems reached 20 % and 45 % efficiencies. Approximately 111 MJ/kg of thermal energy was released by burning 1 kg_{H_2} in an O_2 environment. Syngas production was favoured by higher reaction temperature and residence time and lower feedstock particle size. The use of recovery heat in saltwater desalination instead of solar systems makes the developed system applicable for regions with high wind speeds and low sunlight, as well as areas with low wind speeds and long sunny days. The developed system recommends a pilot-scale development, as current methods of managing and processing plastic waste harm the environment and marine organisms.

CRediT authorship contribution statement

Linus Onwuemezie: Software, Methodology, Conceptualization, Data curation, Formal analysis, Investigation, Validation, Visualization, Writing – original draft, Writing – review & editing. **Hamidreza Gohari Darabkhani:** Data curation, Formal analysis, Writing – review & editing, Conceptualization, Methodology, Supervision.

Declaration of competing interest

The authors declare that they have no known competing financial interests or personal relationships that could have appeared to influence the work reported in this paper.

Data availability

No data was used for the research described in the article.

References

[1] Mojaver M, Hasanzadeh R, Azdast T, Park CB. Comparative study on air gasification of plastic waste and conventional biomass based on coupling of AHP/TOPSIS multi-criteria decision analysis. Chemosphere 2022;286(3):131867.

[2] Sharma B, Goswami Y, Sharma S, Shekhar S. Inherent roadmap of conversion of plastic waste into energy and its life cycle assessment: a frontrunner compendium. Renew Sustain Energy Rev 2021;146:111070.

[3] Walker TR, Fequet L. Current trends of unsustainable plastic production and micro (nano)plastic pollution. TrAC, Trends Anal Chem 2023;160:116984.

[4] Lu T, Jan K, Chen W-T. Hydrothermal liquefaction of pretreated polyethylene-based ocean-bound plastic waste in supercritical water. J Energy Inst 2022;105: 282–92.

[5] Schwarz A, Lensen S, Langeveld E, Parker L, Urbanus J. Plastics in the global environment assessed through material flow analysis, degradation and environmental transportation. Sci Total Environ 2023;875:162644.

[6] Bishop G, Styles D, Lens PN. Recycling of European plastic is a pathway for plastic debris in the ocean. Environ Int 2020;142:105893.

[7] Li W, Tse H, Fok L. Plastic waste in the marine environment: a review of sources, occurrence and effects. Sci Total Environ 2016;566–567:333–49.

[8] Meijer LJJ, Emmerik TV, Ent RVD, Schmidt C, Lebreton L. More than 1000 rivers account for 80% of global riverine plastic emissions into the ocean. Sci Adv 2021;7 (18).

[9] Lebreton L, Slat B, Ferrari F, Sainte-Rose B, Aitken J, Marthouse R, Hajbane S, Cunsolo S, Schwarz A, Levivier A, Noble K, Debeljak P, Maral H, Schoeneich-Argent R, Brambini R, Reisser J. Evidence that the great Pacific Garbage patch is rapidly accumulating plastic. Sci Rep 2018;8:4666.

[10] Law KL, Starr N, Siegler TR, Jambeck JR, Mallos NJ, Leonard GH. The United States' contribution of plastic waste to land and ocean. Sci Adv 2020;6(44): 2375–548.

[11] Syamsiro M, Saptoadi H, Norsujianto T, Noviasri P, Cheng S, Alimuddin Z, Yoshikawa K. Fuel oil production from municipal plastic wastes in sequential pyrolysis and catalytic reforming reactors. Energy Proc 2014;47:180–8.

[12] Ghenai C, Alamara K, Inayat A. Solar assisted pyrolysis of plastic waste: pyrolysis oil characterization and grid-tied solar PV power system design. Energy Proc 2019; 159:123–9.

[13] Miandad R, Barakat M, Aburiazaiza AS, Rehan M, Nizami A. Catalytic pyrolysis of plastic waste: a review. Process Saf Environ Protect 2016;102:822–38.

[14] Aguado J, Serrano D, Miguel GS, Castro M, Madrid S. Feedstock recycling of polyethylene in a two-step thermo-catalytic reaction system. J Anal Appl Pyrol 2007;79(1–2):415–23.

[15] Auxilio AR, Choo W-L, Kohli I, Srivatsa SC, Bhattacharya S. An experimental study on thermo-catalytic pyrolysis of plastic waste using a continuous pyrolyser. Waste Manag 2017;67:143–54.

[16] Budsaereechai S, Hunt AJ, Ngernyen Y. Catalytic pyrolysis of plastic waste for the production of liquid fuels for engines. RSC Adv 2019;9:5844–57.

[17] Hassibi N, Benrabah R, Vega-Bustos YA, Sirjean B, Glaude P-A, Mauviel G, Burklé-Vitzthum V. Oxidative stability of hydrocarbons produced by pyrolysis of polypropylene. Fuel 2024;358:130121.

[18] Onwuemezie L, Darabkhani HG, Ardekani MM. Integrated solar-driven hydrogen generation by pyrolysis and electrolysis coupled with carbon capture and Rankine cycle. Energy Convers Manag 2023;277:116641.

[19] Leng L, Huang H, Li H, Li J, Zhou W. Biochar stability assessment methods: a review. Sci Total Environ 2019;647:210–22.

[20] Kim H-B, Kim J-G, Kim T, Alessi DS, Baek K. Interaction of biochar stability and abiotic aging: influences of pyrolysis reaction medium and temperature. Chem Eng J 2021;411:128441.

[21] Pilon G, Lavoie J-M. Pyrolysis of switchgrass (Panicum virgatum L.) at low temperatures in N₂ and CO₂ environments; a study on chemical composition of chars extracts and bio-oils. J Anal Appl Pyrol 2013;101:122–31.

[22] Lazaroiu G, Pop E, Negreanu G, Pisa I, Mihaescu L, Bondrea A, Berbece V. Biomass combustion with hydrogen injection for energy applications. Energy 2017;127: 351–7.

[23] Onwuemezie L, Darabkhani H, Thermophotovoltaics G. (TPVs), solar and wind assisted hydrogen production and utilisation in iron and steel industry for low carbon productions. J Clean Prod 2024;443:140893.

[24] Kannah RY, Kavitha S, Preethi Karthikeyan OP, Kumar G, Dai-Viet NV, Banu JR. Techno-economic assessment of various hydrogen production methods – a review. Bioresour Technol 2021;319:124175.

[25] Onwuemezie L, Darabkhani HG. Montazeri-Gh M. Pathways for low carbon hydrogen production from integrated hydrocarbon reforming and water electrolysis for oil and gas exporting countries. Sustain Energy Technol Assessments 2024;61:103598.

[26] Khan MA, Zhao H, Zou W, Chen Z, Cao W, Fang J, Xu J, Zhang L, Zhang J. Recent progresses in electrocatalysts for water electrolysis. Electrochem Energy Rev 2018; 1:483–530.

[27] Ostadi M, Bromberg L, Cohn DR, Gençer E. Flexible methanol production process using biomass/municipal solid waste and hydrogen produced by electrolysis and natural gas pyrolysis. Fuel 2023;334(1):126697.

[28] Ying Z, Geng Z, Zheng X, Dou B, Cui G. Improving water electrolysis assisted by anodic biochar oxidation for clean hydrogen production. Energy 2022;238(B): 121793.

[29] Jia JL, Seitz C, Benck JD, Huo Y, Chen Y, Ng JWD, Bilir T, Harris JS, Jaramillo TF. Solar water splitting by photovoltaic-electrolysis with a solar-to-hydrogen efficiency over 30. Nat Commun 2016;7:13237.

[30] Paul B, Andrews J. Optimal coupling of PV arrays to PEM electrolysers in solar–hydrogen systems for remote area power supply. Int J Hydrogen Energy 2008;33(2):490–8.

[31] Burton N, Padilla R, Rose A, Habibullah H. Increasing the efficiency of hydrogen production from solar powered water electrolysis. Renew Sustain Energy Rev 2021; 135:110255.

[32] Oh D, Lee HW, Kim Y-M, Park Y-K. Catalytic pyrolysis of polystyrene and polyethylene terephthalate over Al-MSU-F. Energy Proc 2018;144:111–7.

[33] Kumar S, Singh RK. Recovery of hydrocarbon liquid from waste high density polyethylene by thermal pyrolysis. Braz J Chem Eng 2011;28(4):659–67.

[34] Gao H, Li J. Thermogravimetric analysis of the cocombustion of coal and polyvinyl chloride. PLoS One 2019;14(10):e0224401.

[35] Chaudhary A, Lakhani J, Dalsaniya P, Chaudhary P, Trada A, Shah NK, Upadhyay DS. Slow pyrolysis of low-density Poly-Ethylene (LDPE): a batch experiment and thermodynamic analysis. Energy 2023;263(Part B):125810.

[36] Wang Z, Liu X, Burra KG, Li J, Zhang M, Lei T, Gupta AK. Towards enhanced catalytic reactivity in CO₂-assisted gasification of polypropylene. Fuel 2021;284: 119076.

[37] Kanagasakthivel B, Devaraj D. Simulation and performance analysis of Solar PV-Wind hybrid energy system using MATLAB/SIMULINK. Chennai: IEEE; 2015.

[38] Bouzguenda M, Salmi T, Gastli A, Masmoudi A. Evaluating solar photovoltaic system performance using MATLAB. Nabeul: IEEE; 2012.

[39] Verhelst S, Sierens R. Hydrogen engine-specific properties. Int J Hydrogen Energy 2001;26(9):987–90.

[40] Abdel-Aal H, Sadik M, Bassyouni M, Shalabi M. A new approach to utilize Hydrogen as a safe fuel. Int J Hydrogen Energy 2005;30(13 – 14):1511–4.

[41] Jo Y-D, Crowl DA. Explosion characteristics of hydrogen-air mixtures in a spherical vessel. Process Saf Prog 2010;29(3):216–23.

[42] Rosha P, Kumar S, Ibrahim H. Sensitivity analysis of biomass pyrolysis for renewable fuel production using Aspen Plus. Energy 2022;247:123545.

[43] Luo S, Xiao B, Hu Z, Liu S. Effect of particle size on pyrolysis of single-component municipal solid waste in fixed bed reactor. Int J Hydrogen Energy 2010;35(1): 93–7.

[44] Kohlheb N, Wluka M, Bezama A, Thrän D, Aurich A, Arno R. Environmental-economic assessment of the pressure swing adsorption biogas upgrading technology. BioEnergy Research 2020;14:901–9.

[45] Hasan M, Rasul M, Jahirul M, Sattar M. An Aspen plus process simulation model for exploring the feasibility and profitability of pyrolysis process for plastic waste management. J Environ Manag 2024;355:120557.

[46] Onwuemezie L, Darabkhani HG. Biohydrogen production from solar and wind assisted AF-MEC coupled with MFC, PEM electrolysis of H₂O and H₂ fuel cell for small-scale applications. Renew Energy 2024;224:120160.

[47] Park K-B, Jeong Y-S, Guzelciftci B, Kim J-S. Characteristics of a new type continuous two-stage pyrolysis of waste polyethylene. Energy 2019;166:343–51.

[48] Shehzad A, Bashir MJ, Sethupathi S. System analysis for synthesis gas (syngas) production in Pakistan from municipal solid waste gasification using a circulating fluidized bed gasifier. Renew Sustain Energy Rev 2016;60:1302–11.

[49] Hoekman SK, Robbins C. Review of the effects of biodiesel on NOx emissions. Fuel Process Technol 2012;96:237–49.

[50] Pilon G, Lavoie J-M. Pyrolysis of switchgrass (Panicum virgatum L.) at low temperatures within N2 and CO₂ environments: product yield study. ACS Sustainable Chem Eng 2013;1:198–204.

[51] Parthasarathy P, Al-Ansari T, Mackey HR, McKay G. Effect of heating rate on the pyrolysis of camel manure. Biomass Convers Biorefin 2023;13:6023–35.

[52] Al-Rumaihi A, Shahbaz M, Mckay G, Al-Ansari T. Investigation of co-pyrolysis blends of camel manure, date pits and plastic waste into value added products using Aspen Plus. Fuel 2023;340:127474.

[53] Hasan M, Rasul M, Mofijur M. Fuelling the future: unleashing energy and exergy efficiency from municipal green waste pyrolysis. Fuel 2024;357(A):129815.

[54] Cui L, Ahmad F, Zhang Y, Liu W, Niżetić S. High-quality oil recovered from waste solar panel through using microwave-assisted pyrolysis. Sol Energy 2024;267: 112239.

[55] Onwuemezie L, Darabkhani HG. Solar and wind assisted biohydrogen production from integrated anaerobic digestion and microbial electrolysis cell coupled with catalytic reforming. Energy Convers Manag 2024;305:118224.

[56] Sánchez-Bastardo N, Schlögl R, Ruland H. Methane pyrolysis for zero-emission hydrogen production: a potential bridge technology from fossil fuels to a renewable and sustainable hydrogen economy. Ind Eng Chem Res 2021;60(32):11855–81.

[57] Li J, Wei Y-M, Liu L, Li X, Yan R. The carbon footprint and cost of coal-based hydrogen production with and without carbon capture and storage technology in China. J Clean Prod 2022;362:132514.

[58] Sapountzi FM, Gracia JM, Weststrate C-J, Fredriksson HO, Niemantsverdriet J. Electrocatalysts for the generation of hydrogen, oxygen and synthesis gas. Prog Energy Combust Sci 2017;58:1–35.

[59] Ozgener O. A small wind turbine system (SWTS) application and its performance analysis. Energy Convers Manag 2006;47(11 − 12):1326–37.

[60] Maghami MR, Hizam H, Gomes C, Radzi MA, Rezadad MI, Hajighorbani S. Power loss due to soiling on solar panel: a review. Renew Sustain Energy Rev 2016;59: 1307–16.

[61] Li C, Zhang C, Gholizadeh M, Hu X. Different reaction behaviours of light or heavy density polyethylene during the pyrolysis with biochar as the catalyst. J Hazard Mater 2020;399:123075.

[62] Khoo HH. LCA of plastic waste recovery into recycled materials, energy and fuels in Singapore. Resour Conserv Recycl 2019;145:67–77.

[63] Younas M, Shafique S, Hafeez A, Javed F, Rehman F. An overview of hydrogen production: current status, potential, and challenges. Fuel 2022;316:123317.

[64] Wright MM, Satrio JA, Brown RC, Daugaard DE, Hsu DD. Techno-economic analysis of biomass fast pyrolysis to transportation fuels. Colorado: NREL; 2008.

[65] Alderson H, Cranston GR, Hammond GP. Carbon and environmental footprinting of low carbon UK electricity futures to 2050. Energy 2012;48(1):96–107.